Journal of Molecular Structure 985 (2011) 75–81

Contents lists available at ScienceDirect

Journal of Molecular Structure

journal homepage: www.elsevier.com/locate/molstruc

Crystal and molecular structure of three biologically active nitroindazoles

Pilar Cabildo [a], Rosa M. Claramunt [a,*], Concepción López [a], M. Ángeles García [a], Marta Pérez-Torralba [a], Elena Pinilla [b], M. Rosario Torres [b], Ibon Alkorta [c], José Elguero [c]

[a] Departamento de Química Orgánica y Bio-Orgánica, Facultad de Ciencias, UNED, Senda del Rey 9, E-28040 Madrid, Spain
[b] Departamento de Química Inorgánica I, CAI de Difracción de Rayos-X, Facultad de Ciencias Químicas, Universidad Complutense de Madrid, 28040 Madrid, Spain
[c] Instituto de Química Médica, CSIC, Centro de Química Orgánica Manuel Lora-Tamayo, Juan de la Cierva 3, E-28006 Madrid, Spain

ARTICLE INFO

Article history:
Received 7 September 2010
Received in revised form 13 October 2010
Accepted 13 October 2010
Available online 20 October 2010

Keywords:
NOS
Indazoles
Halogen bond
Hydrogen bonding
NMR
DFT calculations

ABSTRACT

3-Bromo-1-methyl-7-nitro-1*H*-indazole (**1**), 3-bromo-2-methyl-7-nitro-2*H*-indazole (**2**) and 3,7-dinitro-1(2)*H*-indazole (**3**) have been synthesized and characterized by X-ray diffraction, ^{13}C and ^{15}N NMR spectroscopy in solution and in solid-state. The dihedral angles obtained in the crystal structures are in good agreement with the molecular parameters calculated using DFT B3LYP calculations employing the 6-311++G(d,p) basis set. Compounds **1** and **2** present intermolecular halogen bonds between the bromine and the oxygen atoms of the nitro group and in compound **3** inter- and intramolecular hydrogen bonding exists.

1. Introduction

C-nitroindazoles unsubstituted on the N atom, particularly 7-nitro derivatives, are one the most potent families of nitric oxide synthase (NOS) inhibitors. These enzymes catalyze the oxidation of L-arginine to L-citrulline and nitric oxide (NO), a molecule that plays an important role in the regulation of blood pressure, neurotransmission, and the immune response [1]. We have been actively working on these and other indazoles in two directions: first, in their structural aspects related to N–H···N hydrogen bonds and prototropic tautomerism [2–6]; second, in their biological properties [7–9].

We will describe in this paper the structure and spectroscopic properties of three 7-nitroindazole derivatives (Scheme 1): 3-bromo-1-methyl-7-nitro-1*H*-indazole (**1**), 3-bromo-2-methyl-7-nitro-2*H*-indazole (**2**) and 3,7-dinitro-1(2)*H*-indazole (**3**) (1*H*-tautomer **3a** and 2*H*-tautomer **3b**).

The three compounds are known but their synthesis has been reported in several papers not citing comprehensively the literature. The starting material is commercial 7-nitro-1*H*-indazole (**4**) (Scheme 2). Bromination in acetic acid to afford **5** was reported by Auwers and Demuth in 1927 [10]. Treatment of **4** with methyl sulfate in basic conditions yields both *N*-methyl isomers **6** and **7** that can be easily separated [11–13]. Bromination of **6** and **7** affords **1** and **2** [11,12]. The same compounds are obtained by methylation of **5** resulting in a 70/30 ratio of **1/2** [12]. With slightly different conditions, only **1** was obtained [14,15]. 3,7-Dinitro-1(2)*H*-indazole (**3**) was first reported by Habraken and Cohen-Fernandes in 1971 in a two-step procedure through the rather unstable 2-nitro derivative **8** [16]. Compound **3** has been prepared two more times by Wrzeciono, but always with the same procedure [17,18].

2. Results and discussion

2.1. X-ray structures

An X-ray study of compounds **1**, **2** and **3** has been carried out. Figs. 1–3 show the molecular structure for the three compounds. In all cases, the indazole rings are almost planar including the nitro groups in the best least-square plane for **2** and **3** (maximum dihedral angle about 7°), while for **1** the dihedral angle is about 30°.

For **1** and **2** intermolecular halogen bonding [19,20] between the bromine and the oxygen atoms of the nitro group led to chains parallels to axes *c* and *a*, respectively (Figs. 4 and 5). In the case of **1** the interaction involves only one O atom while in the case of **2** the halogen bond is bifurcated (three-centered) and both O atoms of the nitro group contact with the Br atom. Both situations, the first one more common, have been described in the literature [21–23].

* Corresponding author. Tel.: +34 913987322; fax: +34 913988372.
E-mail address: rclaramunt@ccia.uned.es (R.M. Claramunt).

0022-2860/$ - see front matter © 2010 Elsevier B.V. All rights reserved.
doi:10.1016/j.molstruc.2010.10.023

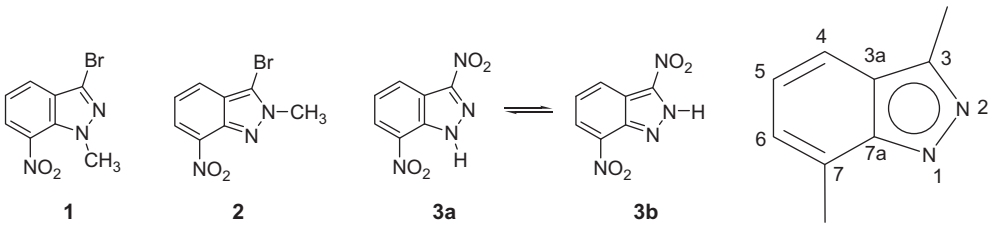

Scheme 1. The three nitroindazoles and the numbering scheme.

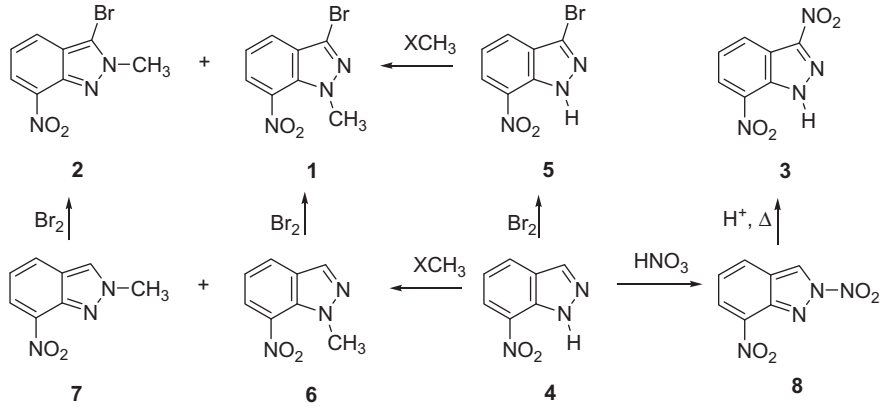

Scheme 2. Synthesis of compounds **1**, **2** and **3**.

In compound **3** bifurcated inter and intramolecular hydrogen bonds form zig-zag chains parallels to axis *a* (Fig. 6). The existence of bifurcated (three-centered) hydrogen bonds had also been reported [24], with some examples involving the nitro group [25–27].

Bond lengths and angles including the hydrogen bonds and electrostatic interactions are collected en Table 1.

2.2. Solution and solid-state NMR

The NMR results are reported in Table 2 (solution) and 3 (solid-state). The assignments of all the signals to the corresponding nuclei have been straightforward and are in agreement with literature data reported for other indazoles [28–30].

The experimental CPMAS NMR spectra reported in Fig. 7 deserve special attention in what concerns their high resolution leading to the observation of all carbon and nitrogen atoms.

2.3. Theoretical calculations

2.3.1. Geometries [B3LYP/6-311++G(d,p)]

According to the calculations, the dihedral angle of the 7-nitro group is 30° for **1** and 0° for **2**, which is expected due to the proximity of the methyl group in **1**. In compound **3** both nitro groups

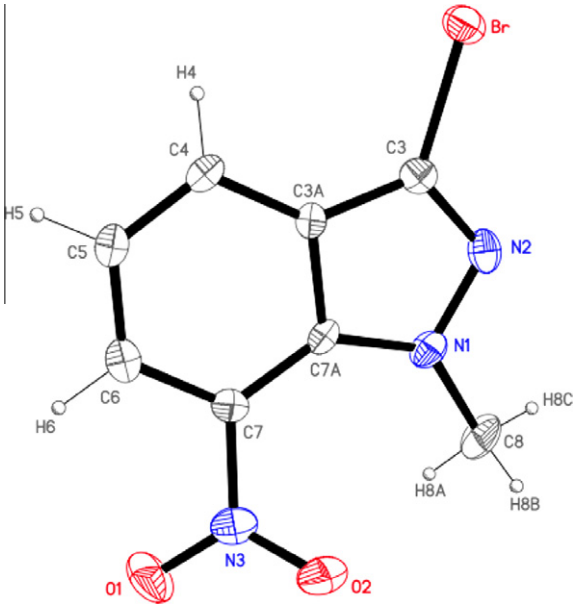

Fig. 1. ORTEP plot (30% probability for the ellipsoids) of **1** showing the labeling of the asymmetric unit.

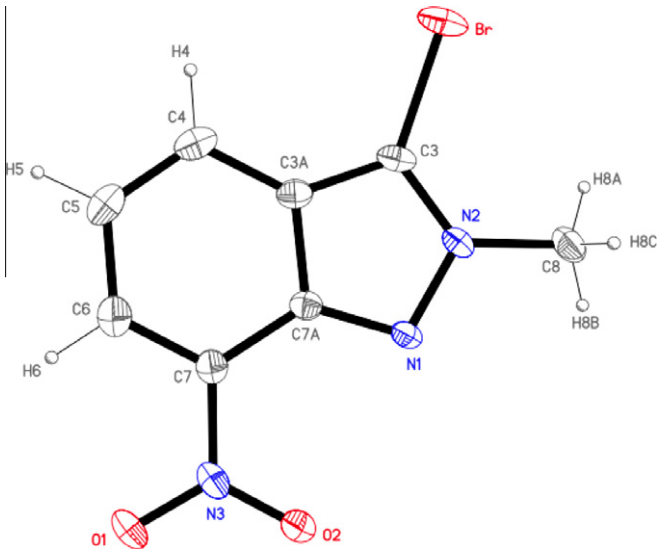

Fig. 2. ORTEP plot (30% probability for the ellipsoids) of **2** showing the labeling of the asymmetric unit.

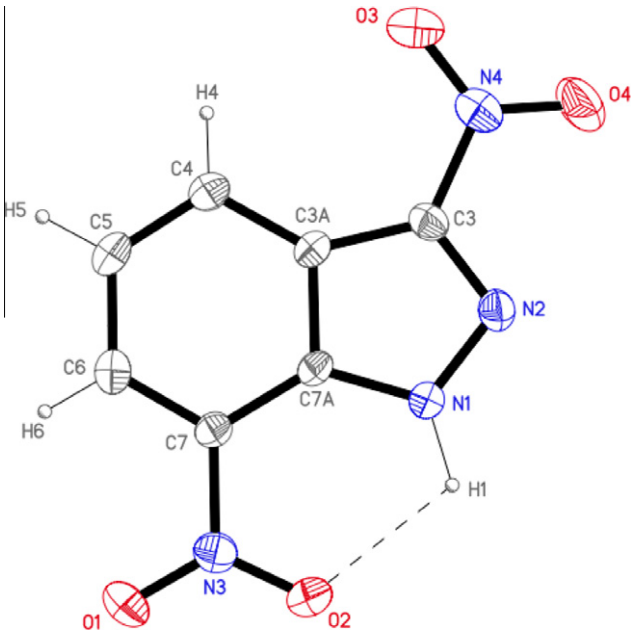

Fig. 3. ORTEP plot (30% probability for the ellipsoids) of **3** showing the labeling of the asymmetric unit. Dotted lines are used to express the intramolecular hydrogen bond.

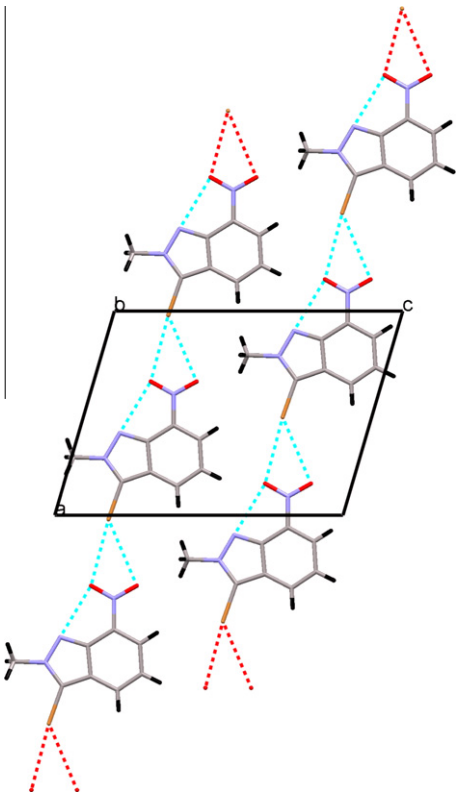

Fig. 5. View along the *b* axis showing the Br–O interactions in compound **2**.

are in the plane of the ring (dihedral angles = 0°). These observations coincide with those reported in the crystallographic section.

2.3.2. Energies [B3LYP/6-311++G(d,p)]

It is well known that in indazoles 1*H*-tautomers (benzenoid) are more stable than 2*H*-tautomers (quinonoid) [31]. This is also the case for compound **3** where 1*H* (**3a**) is 42.5 kJ mol^{-1} more stable than 2*H* (**3b**). The same applies to the isomerism of *N*-substituted derivatives and so the 1-methyl isomer **1** is 19.2 kJ mol^{-1} more stable than the 2-methyl isomer **2**.

2.3.3. NMR [GIAO/B3LYP/6-311++G(d,p)]

The absolute shieldings (σ, ppm) provided by the GIAO calculations can be transformed to chemical shifts (δ, ppm) by means of three empirical equations statistically obtained from large collections of data: $\delta^{13}C = 175.7–0.963 * \sigma^{13}C$ [32], $\delta^{15}N = -152.0–0.946 * \sigma^{15}N$ [32] and $\delta^{1}H = 31.0–0.970 * \sigma^{1}H$ [33]. We have compared the chemical shifts thus obtained with the experimental data for compounds **1** and **2** and the agreement has proved to be excellent (both solution and solid-state) save for the ^{13}C chemical shifts of carbon C-3, the one bearing a bromine substituent. In these cases, the difference exp.–calc. is between −15 and −20 ppm, as we have already reported (−20 ppm [34]).

As we have calculated both tautomers of **3**, in Fig. 8 are reported the signals most sensitive to tautomerism. Only the chemical shifts of **3a** are consistent with the experimental data reported in Tables 2 and 3, those of **3b** being rather different. This is the result expected both from energy considerations and from the X-ray structure for the solid-state, where only one tautomer is found (Fig. 3). The solution data indicate that a low amount, if any, of tautomer **3b** is present. A linear combination of the calculated values for **3a** (94%) and **3b** (6%) afford values very close to the experimental ones.

3. Conclusions

Single-crystal X-ray diffraction analyses indicate that the investigated compounds **1**, **2** and **3** crystallize in the orthorhombic Pbca, monoclinic P2(1)/c and orthorhombic P2(1)2(1)2(1) space groups,

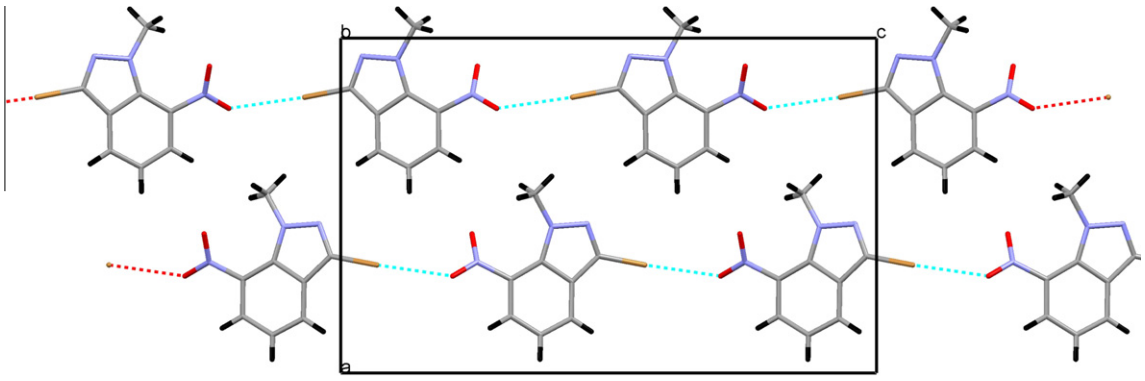

Fig. 4. View along the *b* axis showing the Br–O interactions in compound **1**.

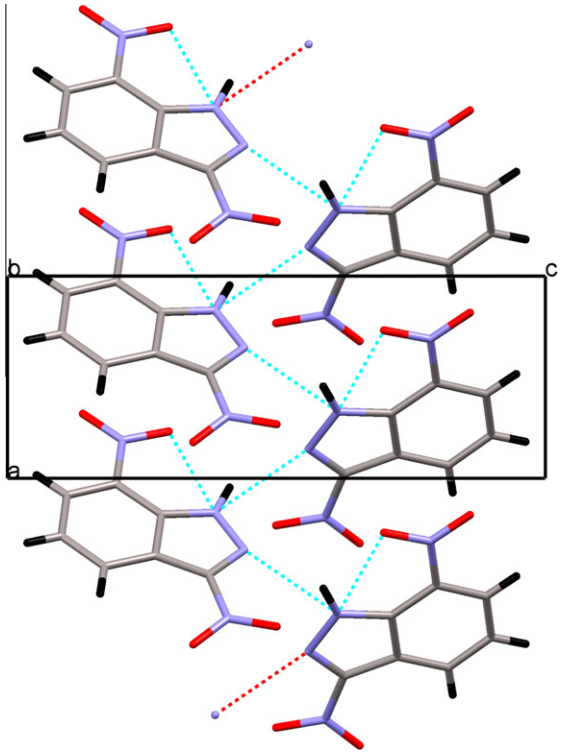

Fig. 6. View along the *b* axis showing the zig-zag chain and the H-bonds in compound **3**.

Table 1
Halogen bond interactions (Å and °) for **1** and **2** and hydrogen bonds (Å and °) for **3**.

Compound	Interactions	Symmetry operations	*d*(Br–O)
1	Br···O1	$x, -y+1/2, z-1/2$	3.089(1)
2	Br···O1	$x-1, y, z$	2.357(1)
2	Br···O2	$x-1, y, z$	2.194(1)

	D–H···A		*d*(D–H)	*d*(H···A)	*d*(D···A)	∠(DHA)
3	N1–H1···O2		1.04	2.15	2.708(3)	111.7
3	N1–H1–N2′	$x-1/2, -y+1/2, -z+1$	1.04	2.21	3.019(3)	133.8

respectively. There is an excellent agreement between experimental (both solution and solid-state) and theoretically calculated ^{13}C and ^{15}N NMR chemical shifts, save for the C-3 chemical shifts in compounds **1** and **2**. DFT calculations predict that the 1-methyl isomer **1** is more stable than the 2-methyl one **2** in 19.2 kJ mol^{-1}, and from the two tautomers 1*H*- and 2*H*- in compound **3**, the first form is stabilized over the latter in about 42.5 kJ mol^{-1}.

4. Experimental section

4.1. Chemistry

Melting points for compounds **1–3** were determined by DSC on a Seiko DSC 220C connected to a Model SSC5200H Disk Station. Thermograms (sample size 0.003–0.0010 g) were recorded at the scanning rate of 2.0 °C min^{-1}. Thin-layer chromatography (TLC) was performed with Merck silica gel (60 F254). Compounds were detected with a 254-nm UV lamp. Silica gel (60–320 mesh) was employed for routine column chromatography separations with the indicated eluent.

3- Bromo-7-nitro-1*H*-indazole (**5**) was prepared according to the published procedure [12].

Table 2
^{13}C and ^{15}N chemical shifts (δ in ppm) and coupling constants (J in Hz).

Nuclei	**1** DMSO-d_6 300 K	**2** DMSO-d_6 300 K	**3** CD_3CN 300 K	**3** THF-d_8 207 K
C3	121.1 (d) ^3J = 4.0	111.0 (m)	151.5 (m)	150.8
C3a	127.3 (d) ^2J = 9.4	124.9 (d) ^2J = 9.2	120.2 (d) ^2J = 9.5	119.7
C4	127.2 (dd) ^1J = 167.0 ^3J = 8.5	128.3 (dd) ^1J = 166.5 ^3J = 8.1	130.3 (dd) ^1J = 171.7 ^3J = 8.6	129.9
C5	121.2 (d) ^1J = 168.8	120.8 (d) ^1J = 167.4	126.4 (d) ^1J = 168.7	125.8
C6	126.0 (ddd) ^1J = 167.2 ^2J = 2.9, ^3J = 7.7	125.9 (ddd) ^1J = 167.4 ^2J = 2.9, ^3J = 9.5	126.8 (ddd) ^1J = 168.5 ^2J = 2.3, ^3J = 8.6	126.0
C7	135.0 (d) ^3J = 9.2	136.4 (d) ^3J = 7.7	134.9 (m)	134.8
C7a	131.9 (dd) ^3J = ^3J = 6.9	139.3 (dd) ^3J = ^3J = 6.9	135.4 (dd) ^3J = ^3J = 6.7	135.1
Me	40.9 (q) ^1J = 142.5	39.5 (q) ^1J = 142.0	–	–
N1	−198.9	−87.1	−199.7[a]	−200.0[a]
N2	−53.6	−155.2	−64.2[a]	−63.3[a]
NO_2	−11.3[a]	−11.3[a]	−21.5[a] (NO_2-3) −14.3[a] (NO_2-7)	−24.6[a] (NO_2-3) −17.1[a] (NO_2-7)

[a] To obtain these ^{15}N NMR chemical shifts the use of a 5-mm inverse detection QNP probe equipped with a *z*-gradient coil, at 333 K for **1** and **2** and 300 K for **3**, was necessary; d: doublet; m: multiplet; q: quartet.

4.1.1. 3-Bromo-1-methyl-7-nitro-1H-indazole (*1*) and 3-bromo-2-methyl-7-nitro-2H-indazole (*2*)

In a round-bottomed flask equipped with reflux condenser, 3-bromo-7-nitro-1*H*-indazole (**5**) (0.63 g, 2.6 mmol) was dissolved in dry methanol (25 mL). Then, sodium methoxyde (0.18 g, 3.3 mmol) and 0.55 g of methyl iodide (0.24 mL, 3.9 mmol) were added. The mixture was heated to reflux for 2 days and then the solvent was removed under reduced pressure. Water (30 mL) was added and the residue was extracted with chloroform (3 × 45 mL). The organic layers were combined, dried (Na_2SO_4), and concentrated to afford a crude solid formed mainly by the two isomers. After silica gel chromatography with (hexane/ethyl acetate 30:1), **1** was obtained first (0.24, 37%) and increasing to 1:1 to afford **2** (0.29, 44%); m.p. (**1**): 161.1 °C (160–162 °C) [12]; m.p. (**2**): 200.5 °C (194–196 °C) [12].

(**1**) ^1H NMR (DMSO-d_6) δ 8.28 (dd, ^3J = 7.9, ^4J = 0.7, 1H, H6), 8.03 (dd, ^3J = 7.9, ^4J = 0.7, 1H, H4), 7.43 (dd, ^3J = ^3J = 7.9, 1H, H5), 4.13 (s, 3H, CH_3); (**2**) ^1H NMR (DMSO-d_6) δ 8.35 (dd, ^3J = 7.9, ^4J = 0.8, 1H, H6), 8.02 (dd, ^3J = 7.9, ^4J = 0.8, 1H, H4), 7.31 (dd, ^3J = ^3J = 7.9, 1H, H5), 4.24 (s, 3H, CH_3).

4.1.2. 3,7-Dinitro-1H(2H)-indazole (*3*)

This compound was prepared according to Ref. [16] and obtained as a yellow solid. M.p. 221.8 °C; m.p. 220 °C [16]. ^1H NMR (CD_3CN) δ 12.83 (br s, 1H, NH), 7.65 (t, ^3J = 8.0, 1H, H5), 8.48 (d, ^3J = 7.9, 1H, H6), 8.62 (d, ^3J = 8.1, 1H, H4).

4.2. NMR spectroscopy

Solution spectra were recorded at 300 K on a Bruker DRX 400 (9.4 T, 400.13 MHz for ^1H, 100.62 MHz for ^{13}C and 40.56 MHz for ^{15}N) spectrometer with a 5-mm inverse detection H–X probe equipped with a *z*-gradient coil for ^1H, ^{13}C and ^{15}N, save specified. Chemical shifts (δ in ppm) are given from internal solvents, DMSO-d_6 (2.49) and CD_3CN (1.93) for ^1H and DMSO-d_6 (39.5) and CD_3CN (118.7) for ^{13}C. And external reference $CH_3{}^{15}NO_2$ (0.00) for ^{15}N NMR was used. 2D (^1H–^1H) gs-COSY and inverse proton detected

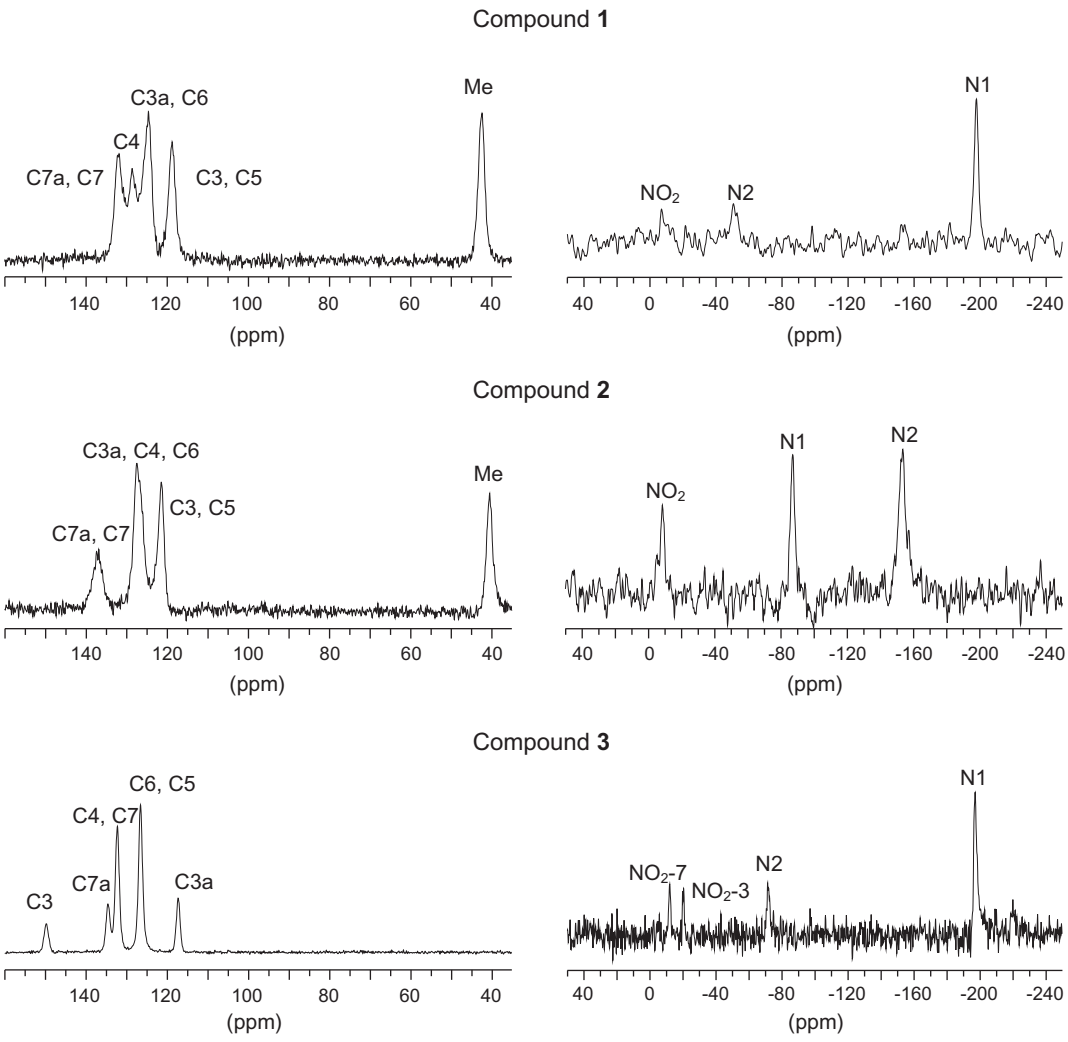

Fig. 7. The ^{13}C and ^{15}N CPMAS NMR spectra of compounds **1**–**3**.

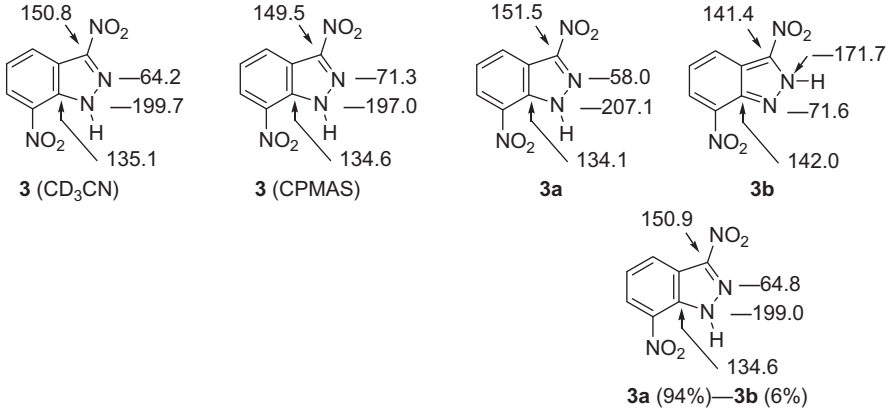

Fig. 8. The tautomerism of 3,7-dinitro-1(2)*H*-indazole (**3**). Experimental results in solution and in the solid-state *vs.* calculated values in the gas phase.

heteronuclear shift correlation spectra, (^1H–^{13}C) gs-HMQC, (^1H–^{13}C) gs-HMBC, (^1H–^{15}N) gs-HMQC, and (^1H–^{15}N) gs-HMBC, were acquired and processed using standard Bruker NMR software and in non-phase-sensitive mode [35]. Gradient selection was achieved through a 5% sine truncated shaped pulse gradient of 1 ms. Variable temperature experiments were recorded on the same spectrometer. A Bruker BVT3000 temperature unit was used to control the temperature of the cooling gas stream and an exchanger to achieve low temperatures.

Solid state ^{13}C (100.73 MHz) and ^{15}N (40.60 MHz) CPMAS NMR spectra have been obtained on a Bruker WB 400 spectrometer at 300 K using a 4 mm DVT probehead and a 4-mm diameter cylindrical zirconia rotor with Kel-F end-caps. The non-quaternary suppression (NQS) technique to observe only the quaternary carbon

Table 3
^{13}C and ^{15}N chemical shifts (δ in ppm) in solid-state (CPMAS, 300 K).

Comp.	C3	C3a	C4	C5	C6	C7	C7a	Me	N1	N2	NO_2
1	118.7	126.0	128.6	118.7	124.6	132.2	131.8	42.4	−197.8	−50.6	−7.0
2	121.5	127.5	127.5	121.5	127.5	136.5	138.0	40.5	−87.1	−153.5	−8.4
3	149.5	117.5	132.3	126.3	126.3	132.3	134.6	–	−197.0	−71.3	−12.0 (NO_2-7) −20.5 (NO_2-3)

Table 4
Crystal data and structure refinement for compounds **1**, **2** and **3**.

Crystal Data	**1**	**2**	**3**
Identification code	CCDC – 780744	CCDC – 780745	CCDC – 780746
Empirical formula	$C_8H_6BrN_3O_2$	$C_8H_6BrN_3O_2$	$C_7H_4N_4O_4$
Formula weight	256.07	256.07	208.14
Wavelength (Å)	0.71073	0.71073	0.71073
Crystal system	Orthorhombic	Monoclinic	Orthorhombic
Space group	Pbca	P2(1)/c	P2(1)2(1)2(1)
Unit cell dimensions			
a (Å)	12.705(2)	9.882(2)	4.9853(7)
b (Å)	6.994(1)	7.111(2)	12.265(2)
c (Å)	20.436(3)	13.357(3)	13.265(2)
β (°)	–	−106.255(4)	–
Volume (Å^3)	1808.0(5)	901.0(3)	811.1(2)
Z	8	4	4
Density (calculated) (Mg/m^3)	1.881	1.888	1.713
Absorption coefficient	4.522 (mm^{-1})	4.537 (mm^{-1})	0.144 (mm^{-1})
F(0 0 0)	424	504	424
Theta range (°) for data collection	2.23–25.0	2.29–25.0	2.26–25.00
Index ranges	$-15\leqslant h\leqslant 13$ $-8\leqslant k\leqslant 8$ $-24\leqslant l\leqslant 24$	$-11\leqslant h\leqslant 11$ $-8\leqslant k\leqslant 8$ $-14\leqslant l\leqslant 15$	$-5\leqslant h\leqslant 5$ $-14\leqslant k\leqslant 12$ $-14\leqslant l\leqslant 15$
Reflections collected	12,237	6300	6204
Independent reflec. [*R*(int)]	1594 [0.0532]	1580 [0.0448]	1422 [0.0654]
Data/restraints/parameters	1594/0/128	1580/0/127	1422/0/137
Goodness-of-fit on F^2	1.012	1.006	0.833
R[a][$I > 2$sigma(I)] (obs. reflec.)	0.0776 (1185)	0.0304 (1070)	0.0328(885)
Rw_F [b] (all data)	0.2180	0.0921	0.0703

[a] $\sum||F_o|-|F_c||/\sum|F_o|$.
[b] $\{\sum[w(F_o^2-F_c^2)^2]/\sum[w(F_o^2)^2]\}^{1/2}$.

atoms was employed [35]. ^{13}C spectra were originally referenced to a glycine sample and then the chemical shifts were recalculated to the Me_4Si (for the carbonyl atom δ (glycine) = 176.1 ppm) and ^{15}N spectra to $^{15}NH_4Cl$ and then converted to nitromethane scale using the relationship: δ ^{15}N(nitromethane) = δ ^{15}N(ammonium chloride) – 338.1 ppm.

4.3. X-ray data collection and structure refinement for compounds *1*, *2* and *3*

Suitable crystals for X-ray diffraction experiments were obtained by crystallization from acetone–water for **1**, from ethyl acetate–hexane for **2** and from tetrahydrofurane for **3**. Data collection for all compounds was carried out at room temperature on a Bruker Smart CCD diffractometer using graphite-monochromated Mo Kα radiation (λ = 0.71073 Å) operating at 50 kV and 30 mA. In all cases, the data were collected over a hemisphere of the reciprocal space by combination of three exposure sets. Each frame exposure time was 20 s, covering 0.3° in ω. The cell parameters were determined and refined by least-squares fit of all reflections collected. The first 100 frames were recollected at the end of the data collection to monitor crystal decay, and no appreciable decay was observed. An empirical absorption correction was applied for **1** and **2** compounds. A summary of the fundamental crystal and refinement data is given in Table 4. The structures of all the compounds were solved by direct methods and refined by full-matrix least-squares on F^2 (SHELXL-97). All non-hydrogen atoms were refined anisotropically. In all cases the hydrogen atoms were included with fixed isotropic contributions at their calculated positions determined by molecular geometry except for the H1 bonded to N1 for **3**, which was located from the Fourier map and included. All hydrogen refined riding on the corresponding bonded atom. All the calculations were carried out with SHELX-97 [36].

4.4. Computational details

Theoretical calculations were carried out within the Gaussian 03 facilities [37]. The geometries were fully optimized at the B3LYP/6-311++G(d,p) level [38,39], and frequency calculations verified its minimum nature. On these geometries GIAO calculations [40] were carried out.

Supplementary material

Crystallographic data for molecules **1**, **2** and **3** have been deposited at the Cambridge Crystallographic Data Center with the deposition numbers CCDC – 780744, CCDC – 780745 and CCDC – 780746. Copies of the data can be obtained free of charge via external link http://ccdc.cam.ac.uk/retrieving.html.

Acknowledgements

This work has been financed by the Spanish MICINN (CTQ2007-62113, CTQ2009-13129-C02-02 and CTQ2010-16122) and Comunidad Autónoma de Madrid (Project MADRISOLAR2, ref S2009/PPQ-1533).

References

[1] R.M.J. Palmer, A.G. Ferrige, S. Moncada, Nature 327 (1987) 524.
[2] C. López, R.M. Claramunt, S. Trofimenko, J. Elguero, Can. J. Chem. 71 (1993) 678.
[3] M.A. García, C. López, R.M. Claramunt, A. Kenz, M. Pierrot, J. Elguero, Helv. Chim. Acta 85 (2002) 2763.
[4] J. Teichert, P. Oulié, K. Jacob, L. Vendier, M. Etienne, R.M. Claramunt, C. López, C. Pérez Medina, I. Alkorta, J. Elguero, New J. Chem. 31 (2007) 936.
[5] C. Pérez Medina, C. López, R.M. Claramunt, J. Elguero, J. Heterocycl. Chem. 46 (2009) 1408.
[6] C. Pérez Medina, C. López, R.M. Claramunt, J. Elguero, Eur. J. Org. Chem. (2010) 890.
[7] R.M. Claramunt, C. López, C. Pérez-Medina, M. Pérez-Torralba, J. Elguero, G. Escames, D. Acuña-Castroviejo, Bioorg. Med. Chem. 17 (2009) 6180.
[8] J. Elguero, I. Alkorta, R.M. Claramunt, C. López, D. Sanz, D. Santa María, Bioorg. Med. Chem. 17 (2009) 8027.
[9] R.M. Claramunt, C. López, A. López, C. Pérez-Medina, M. Pérez-Torralba, I. Alkorta, J. Elguero, G. Escames, D. Acuña-Castroviejo, Eur. J. Med. Chem., submitted for publication.
[10] K. von Auwers, W. Demuth, Ann. Chem. 451 (1927) 295.
[11] R. Sureau, Chimia 15 (1961) 195.
[12] M. Benchidmi, P. Bouchet, R. Lazaro, J. Heterocycl. Chem. 16 (1979) 1599.
[13] P. Bouchet, R. Lazaro, M. Benchidmi, J. Elguero, Tetrahedron 36 (1980) 3523.
[14] L. Bouissane, S.E. Kazzouli, J.M. Léger, C. Jarry, E.M. Rakib, M. Khouili, G. Guillaumet, Tetrahedron 61 (2005) 8218.
[15] B. Cottyn, F. Acher, B. Ramassamy, L. Alvey, M. Lepoivre, Y. Frapart, D. Stuehr, D. Mansuy, J.L. Boucher, D. Vichard, Bioorg. Med. Chem. 16 (2008) 5962.
[16] L. Habraken, P. Cohen-Fernandes, J. Org. Chem. 36 (1971) 3084.
[17] U. Wrzeciono, E. Linkowska, A. Rogowska, M. Lakoma, D. Kubiak, Pharmazie 39 (1984) 389.
[18] J. Usarewicz, U. Wrzeciono, Z. Lukaszewski, R. Gatniejewska, K. Peisert, Pharmazie 47 (1992) 15.
[19] A.C. Legon, Phys. Chem. Chem. Phys. 12 (2010) 7736.
[20] P. Politzer, J.S. Murray, T. Clark, Phys. Chem. Chem. Phys. 12 (2010) 7748.
[21] Y.X. Lu, J.W. Zou, Y.H. Wang, Q.S. Yu, J. Mol. Struct. Theochem 767 (2006) 139.
[22] M. Kubicki, P. Wagner, Acta Crystallogr. Sect. C 63 (2007) o454.
[23] Y.H. Wang, L. Li, Y.X. Lu, J.W. Zou, Chin. J. Chem. Phys. 20 (2007) 531.
[24] L.S. Szczepura, K.K. Eilts, A.K. Hermetet, L.J. Ackerman, J.K. Swearingen, D.X. West, J. Mol. Struct. 607 (2002) 101.
[25] B. Vickery, G.R. Willey, M.G.B. Drew, J. Chem. Soc. Perkin Trans. 2 (1981) 155.
[26] B. Vickery, G.R. Willey, M.G.B. Drew, Acta Crystallogr. Sect. C. 41 (1985) 586.
[27] I.G. Krivoruchka, A.I. Vokin, V.K. Turchaninov, Russ. J. Org. Chem. 38 (2002) 1456.
[28] J. Elguero, A. Fruchier, E.M. Tjiou, S. Trofimenko, Chem. Heterocycl. Compd. (Engl. Ed.) 31 (1995) 1006.
[29] R.M. Claramunt, D. Sanz, C. López, J.A. Jiménez, M.L. Jimeno, J. Elguero, A. Fruchier, Magn. Res. Chem. 35 (1997) 35.
[30] L. Larina, V. Lopyrev, Nitroazoles: Synthesis, Structure and Applications, Springer, Berlin, 2009.
[31] I. Alkorta, J. Elguero, J. Phys. Org. Chem. 18 (2005) 719.
[32] F. Blanco, I. Alkorta, J. Elguero, Magn. Reson. Chem. 45 (2007) 797.
[33] A.M.S. Silva, R.M.S. Sousa, M.L. Jimeno, F. Blanco, I. Alkorta, J. Elguero, Magn. Reson. Chem. 46 (2008) 859.
[34] C.P. Frizzo, M.A.P. Martins, M.R.B. Marzari, P.T. Campos, R.M. Claramunt, M.A. García, D. Sanz, I. Alkorta, J. Elguero, J. Heterocycl. Chem. doi:10.1002/jhet.377.
[35] S. Berger, S. Braun, 200 And More NMR Experiments, Wiley-VCH, Weinheim, 2004.
[36] G.M. Sheldrick, SHELX97, Program for Refinement of Crystal Structure, University of Göttingen, Göttingen, Germany, 1997.
[37] M.J. Frisch, G.W. Trucks, H.B. Schlegel, G.E. Scuseria, M.A. Robb, J.R. Cheeseman, J.A. Montgomery Jr., T. Vreven, K.N. Kudin, J.C. Burant, J.M. Millam, S.S. Iyengar, J. Tomasi, V. Barone, B. Mennucci, M. Cossi, G. Scalmani, N. Rega, G.A. Petersson, H. Nakatsuji, M. Hada, M. Ehara, K. Toyota, R. Fukuda, J. Hasegawa, M. Ishida, T. Nakajima, Y. Honda, O. Kitao, H. Nakai, M. Klene, X. Li, J.E. Knox, H.P. Hratchian, J.B. Cross, C. Adamo, J. Jaramillo, R. Gomperts, R.E. Stratmann, O. Yazyev, A.J. Austin, R. Cammi, C. Pomelli, J.W. Ochterski, P.Y. Ayala, K. Morokuma, G.A. Voth, P. Salvador, J.J. Dannenberg, V.G. Zakrzewski, S. Dapprich, A.D. Daniels, M.C. Strain, O. Farkas, D.K. Malick, A.D. Rabuck, K. Raghavachari, J.B. Foresman, J.V. Ortiz, Q. Cui, A.G. Baboul, S. Clifford, J. Cioslowski, B.B. Stefanov, G. Liu, A. Liashenko, P. Piskorz, I. Komaromi, R.L. Martin, D.J. Fox, T. Keith, M.A. Al-Laham, C.Y. Peng, A. Nanayakkara, M. Challacombe, P.M.W. Gill, B. Johnson, W. Chen, M.W. Wong, C. Gonzalez, J.A. Pople, Gaussian 03, Gaussian, Inc., Pittsburgh PA, 2003.
[38] A.D. Becke, Phys. Rev. A 38 (1988) 3098;
A.D. Becke, J. Chem. Phys. 98 (1993) 5648;
C. Lee, W. Yang, R.G. Parr, Phys. Rev. B 37 (1988) 785.
[39] P.A. Hariharan, J.A. Pople, Theor. Chim. Acta 28 (1973) 213.
[40] R. Ditchfield, Mol. Phys. 27 (1974) 789;
F. London, J. Phys. Rad. 8 (1937) 397.